



# Proton MRD Profile Analysis in Intracellular Hemoglobin Solutions: A Three Sites Exchange Model Approach

Manuel Arsenio Lores Guevara<sup>1</sup> · Carlos Alberto Cabal Mirabal<sup>1,2</sup> · Robert N. Muller<sup>3</sup> · Sophie Laurent<sup>3</sup> · Fabian Tamayo Delgado<sup>1</sup> · Juan Carlos García Naranjo<sup>1</sup>

Received: 15 September 2021 / Revised: 12 November 2021 / Accepted: 16 November 2021 /  
Published online: 6 January 2022

© The Author(s), under exclusive licence to Springer-Verlag GmbH Austria, part of Springer Nature 2021

## Abstract

The Three Sites Exchange Model (3SEM) was properly used to describe Proton (<sup>1</sup>H) Magnetic Relaxation Dispersion (<sup>1</sup>HMRD) in intracellular samples of hemoglobin A (HbA) and hemoglobin S (HbS) at 310 K. The HbA and HbS samples were obtained from whole blood of voluntary donors and patients, respectively, and processed by classical methods (centrifugation, decanting and freezing–thawing cycles). The <sup>1</sup>HMRD profiles (20 kHz–60 MHz) were obtained using a Fast Field Cycling NMR Relaxometer (Stelar FFC 2000 Spinmaster) and Minispec relaxometers (Mq20, Mq60). The 3SEM used includes the contribution of labile protons from the structure of the protein; and the contribution of the cross relaxation to dispersion was estimated as: at least one order of magnitude lower than the total dispersion. Two dispersions were found: one of them properly describing the hemoglobin rotational correlation time and another one probably related to internal and/or hydrated water molecules with effective correlation times higher than 1 ns and main residence times less than the rotational correlation time of the protein. The use of the 3SEM creates the conditions to properly explain proton magnetic relaxation during the HbS polymerization process.

**Keywords** <sup>1</sup>HMRD profiles · HbA · HbS · HbS polymerization · Three sites exchange model

---

✉ Fabian Tamayo Delgado  
tamayofabio0@gmail.com

<sup>1</sup> Centro de Biofísica Médica, Universidad de Oriente, Patricio Lumumba S/N., CP: 90500, Santiago de Cuba, Cuba

<sup>2</sup> Facultad de Física, Universidad de La Habana, Havana, Cuba

<sup>3</sup> Laboratoire de RMN Et d'Imagerie Moléculaire, Service de Chimie Générale, Organique Et Biomédicale, Faculté de Médecine Et de Pharmacie, Université de Mons, Mons, Belgium

## 1 Introduction

Proton ( $^1\text{H}$ ) Magnetic Relaxation has been successfully used to develop medical applications [1–4] in Sickle Cell Disease (SCD) [5–10]. The behaviors of the transverse ( $T_2$ ) and longitudinal ( $T_1$ ) relaxation times in intracellular hemoglobin (Hb) solutions have allowed to determine the delay time of the hemoglobin S (HbS) polymerization process [1, 2]; giving the possibility of to differentiate the crisis and the steady state in SCD patients [2], as well as to evaluate a potential treatment [1, 2, 4]. To explain these  $T_1$  and  $T_2$  behaviors a two sites water exchange model (2SWEM) [11–17] was used (see appendix 1) considering an increasing of the Hb rotational correlation time ( $\tau_R$ ) from 50 to 98 ns [1, 2]. Nevertheless, the  $\tau_R$  values obtained for intracellular Hb solutions do not match with the expected values according to the Debye and Mooney models ( $\sim 172$  ns) [18], moreover, this analysis does not consider the behavior of the bound water fraction ( $P_b$ ) during HbS polymerization [15]. On the other hand, the 2SWEM has received a lot of criticism related with its reduced capacity to describe proton relaxation in protein solutions due to the low numbers of sites available for water binding to the protein ( $n_{ws}$ ) obtained using this approach; and because of, this model, predicts a Lorentzian dispersion which is not reproduced experimentally [15, 19]. Additionally, the performed analysis does not take into account the contribution to  $^1\text{H}$  magnetic relaxation due to cross-relaxation neither the contribution from labile protons at the protein structure which exchange with the solvent.

According to what was discussed above, to explain the  $T_1$  and  $T_2$  behaviors during HbS polymerization we need another experimental method to determine  $\tau_R$  and, at least, to estimate the  $P_b$  behavior. Also we need another physical approach to describe relaxation, which must includes the cross relaxation and labile protons contributions.

In this work we have used the  $^1\text{H}$  Magnetic Relaxation Dispersion ( $^1\text{HMRD}$ ) experiment to evaluate  $\tau_R$ , and other parameters directly related to  $P_b$ , in intracellular Hb samples. A three sites exchange model (3SEM), including the contributions of labile protons and cross relaxation, was used as physical approach to describe  $^1\text{H}$  magnetic relaxation. The obtained results create the conditions to perform a proper analysis during HbS polymerization.

## 2 Materials and Methods

Samples of whole blood were obtained from voluntary healthy donors and SCD patients (residual samples from the ULB Brussels University Hospital obtained after routine blood tests were finished). The hemoglobin A (HbA) and HbS samples were prepared from whole blood using classical methods [11, 12, 18, 20, 21] and 500  $\mu\text{l}$  of Hb solution were transferred to a NMR tube for the measurements.

A Fast Field Cycling NMR Relaxometer (Stelar FFC 2000 Spinmaster) was used, in the range from 20 kHz to 10 MHz, to obtain the  $^1\text{HMRD}$  profiles at

310 K, which were represented as semilog plots of  $R_1 (1/T_1)$  versus the Larmour frequency ( $\omega_0$ ) divided by  $2\pi$ . Additional points at 20 MHz and 60 MHz were added after measuring the samples in the Mq20 and Mq60 NMR analyzers (Minispec) from Bruker. For each sample at least five  $^1\text{HMRD}$  profiles were measured and the values of the obtained parameters reported as:  $\bar{u} \pm SD$ . Here  $\bar{u}$  and  $SD$  represent the main value and the standard deviation of the performed measurements.

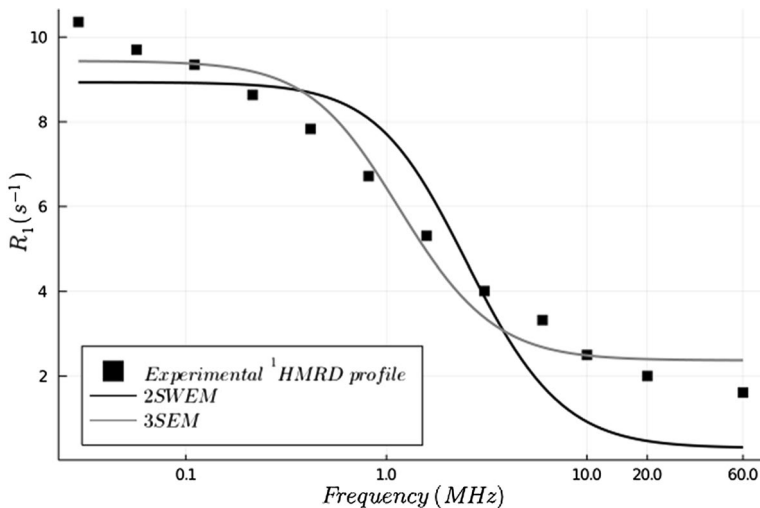
### 3 Results and Discussion

Figure 1 shows the typical  $^1\text{HMRD}$  profile obtained in intracellular Hb solutions at 310 K. The  $^1\text{HMRD}$  profiles were fitted using the Eqs. (1) and (2) corresponding to the 2SWEM and the 3SEM [16, 22–26], respectively (see appendix 1 and 2):

$$R_1(\omega_0) = R_{1w}^{bulk} + P_b \frac{3}{2} \left( \frac{\mu_0}{4\pi} \right)^2 \frac{\gamma^4 \hbar^2}{r^6} \tau_R \left[ \frac{0.2}{1 + \omega_0^2 \tau_R^2} + \frac{0.8}{1 + 4\omega_0^2 \tau_R^2} \right] \quad (1)$$

$$R_1(\omega_0) = R_{1w}^{bulk} + \alpha + \beta \tau_R \left[ \frac{0.2}{1 + (\omega_0 \tau_R)^2} + \frac{0.8}{1 + 4(\omega_0 \tau_R)^2} \right] \quad (2)$$

Here  $R_{1w}^{bulk}$  is the longitudinal magnetic relaxation rate of the  $^1\text{H}$  in the solvent,  $\gamma$  is the  $^1\text{H}$  gyromagnetic ratio,  $\hbar$  is the Planck's constant divided by  $2\pi$ ,  $\mu_0$  is the magnetic permeability of the vacuum and  $r$  is the inter proton distance. In Eq. (2)  $\alpha$  (characterizing the high-frequency relaxation rate plateau) is ascribed to the hydrated water molecules at the protein surface and  $\beta$  (characterizing the magnitude



**Fig. 1** Typical  $^1\text{HMRD}$  profile in intracellular Hb solutions at 310 K. The profile has been fitted using the two sites and three sites exchange models

of the relaxation dispersion) is ascribed to the internal water molecules and the labile protons at the protein structure [22].

The parameters resulting from the fit of the experimental  $^1\text{HMRD}$  profiles to Eq. (2) appear summarized in Table 1.

The values of  $\alpha$ ,  $\beta$  and  $\tau_R$  obtained for intracellular HbA and HbS samples are one order of magnitude bigger than those obtained in previous works for diluted solutions of Bovine Pancreatic Trypsin Inhibitor (BPTI, 6511 Da) by Bertil Halle and co-workers using the same approach [16, 22]. This is a coherent result because Hb is a 64,500 Da protein, which has a major size and a major surface, and also this macromolecule should have a major amount of cavities and deep crevices. These differences could increase the number of water molecules bound to the protein molecule at its surface and in small cavities and deep crevices; as well as the number of labile protons at the macromolecular structure; giving place to the increment of  $\alpha$  and  $\beta$  (see appendix 2). The increasing of  $\tau_R$  could be explained by the increment in size and also by the increasing of protein–protein interactions considering the HbA and HbS concentration [13, 22].  $\beta$  includes the contribution of the labile protons at the protein structure, which has been estimated as 4 times the contribution of internal water molecules for  $pH$  values as used in this work ( $pH = 7.4$ ) [22].

To evaluate the contribution of the cross-relaxation, a negative term ( $-\beta_{cross}\tau_R F_{cross}(\omega_0\tau_R)$ ) was added to the Eq. (2) (see appendix 2) [22], where  $F_{cross}$  is a dispersion function. The fitting of the experimental  $^1\text{HMRD}$  profiles to this modified equation allowed to obtain the values of the dispersion magnitude corresponding to the contribution of the cross-relaxation ( $\beta_{cross}$ ), these values appear summarized in Table 2 for all the studied samples. The values of  $\beta_{cross}$  are, at least, one order of magnitude lower than the values of  $\beta$  (Table 1). Which means that the contribution of cross-relaxation to dispersion can be neglected and Eq. (2) can be used to properly describe  $^1\text{HMRD}$  experimental profiles as in Fig. 1 and Table 1.

The 2SWEM clearly fail to fit the experimental  $^1\text{HMRD}$  profiles (see Fig. 1, adjusted  $r$  square  $\sim 0.7$ – $0.8$ ). To solve this inconvenient, suitable mathematical approaches were developed by Lindstrom and Koenig (LK) [15] and Hallenga and Koenig (HK) [19]:

**Table 1** Parameters obtained from the fit of the experimental  $^1\text{HMRD}$  profiles (310 K) to the 3SEM in intracellular samples of HbA and HbS

Sample	$\alpha$ ( $\text{s}^{-1}$ )	$\beta$ ( $10^8 \text{ s}^{-2}$ )	$\tau_R$ (ns.)	Adjusted $r$ square
HbA-1	$2.17 \pm 0.07$	$0.93 \pm 0.04$	$75.3 \pm 2.6$	$0.96 \pm 0.01$
HbA-2	$2.42 \pm 0.25$	$1.09 \pm 0.20$	$49.3 \pm 9.2$	$0.95 \pm 0.01$
HbA-3	$5.52 \pm 0.05$	$1.27 \pm 0.68$	$66.8 \pm 3.5$	$0.94 \pm 0.003$
HbA-4	$3.84 \pm 0.11$	$1.05 \pm 0.04$	$67.0 \pm 2.1$	$0.95 \pm 0.01$
HbA-5	$4.85 \pm 0.10$	$1.12 \pm 0.05$	$73.4 \pm 3.6$	$0.93 \pm 0.01$
HbA-6	$5.01 \pm 0.01$	$1.03 \pm 0.04$	$74.0 \pm 3.0$	$0.93 \pm 0.003$
HbA-7	$5.72 \pm 0.06$	$1.16 \pm 0.04$	$86.4 \pm 4.3$	$0.95 \pm 0.003$
HbS-1	$1.79 \pm 0.06$	$0.76 \pm 0.04$	$65.9 \pm 2.7$	$0.94 \pm 0.003$
HbS-2	$2.20 \pm 0.05$	$0.85 \pm 0.05$	$60.1 \pm 5.5$	$0.93 \pm 0.01$

**Table 2** Values of  $\beta_{cross}$  obtained fitting the experimental  $^1\text{HMRD}$  profiles of intracellular HbA and HbS samples (310 K) to the Eq. (2) modified adding the term:  $-\beta_{cross}\tau_R F_{cross}(\omega_0\tau_R)$

Sample	HbA-1	HbA-2	HbA-3	HbA-4	HbA-5
$\beta_{cross}$ ( $10^8 \text{ s}^{-2}$ )	$0.04 \pm 0.002$	$0.04 \pm 0.005$	$0.05 \pm 0.002$	$0.04 \pm 0.001$	$0.05 \pm 0.002$
Sample	HbA-6	HbA-7	HbS-1	HbS-2	–
$\beta_{cross}$ ( $10^8 \text{ s}^{-2}$ )	$0.04 \pm 0.001$	$0.05 \pm 0.001$	$0.03 \pm 0.001$	$0.03 \pm 0.001$	–

$$R_1(\omega_0) = \frac{BP_b\sqrt{3}\tau_R}{1 + (\omega_0\sqrt{3}\tau_R)^\lambda} + E \tag{3}$$

$$R_1(\omega_0) = R_{1w}^{bulk} + G + \frac{H\left(1 + \left(\frac{\omega_0}{2\pi\nu_c}\right)^{\frac{\varepsilon}{2}} \cos\left(\frac{\pi\varepsilon}{4}\right)\right)}{1 + 2\left(\frac{\omega_0}{2\pi\nu_c}\right)^{\frac{\varepsilon}{2}} \cos\left(\frac{\pi\varepsilon}{4}\right) + \left(\frac{\omega_0}{2\pi\nu_c}\right)^\varepsilon} \tag{4}$$

where  $B$  represents the magnitude of the proton dipolar interaction and  $E$  includes the relaxation of bulk water as well as other high-frequency contributions to relaxation.  $G$ ,  $\lambda$ ,  $\varepsilon$ ,  $H$  and  $\nu_c$  are parameters obtained from the fit [15, 19]. In the HK approach  $\tau_R = \sqrt{3}/(6\pi\nu_c)$  and in the case of LK model  $\tau_R$  is obtained directly from the fit. The HK model is the most used approach and is commonly known as Cole–Cole expression [19, 27]. Despite its really good description of the  $^1\text{HMRD}$  experimental profiles (see Fig. 2, adjusted  $r$  square  $\sim 0.99$ ), the LK and HK methods have received a lot of criticism because of those models are not properly based on proton magnetic relaxation theory [27].

The 3SEM improved the description of the experimental  $^1\text{HMRD}$  profiles in intracellular Hb solutions (see Fig. 1, adjusted  $r$  square  $\sim 0.95$ ) with respect to the 2SWEM, obtaining a performance comparable with the LK and HK approaches. The cause of the similitude between the 3SEM and the suitable mathematical approaches (LK and HK models) is the presence, in all of these models, of three contributions to relaxation: the bulk water contribution, a non-dispersive term and a dispersive contribution. In the Eq. (3)  $E$  can be divided in bulk water contribution and others high-frequency contributions (non-dispersive term) and in the Eq. (4)  $G$  is the non-dispersive term. Moreover,  $BP_b\sqrt{3}$  and  $H$  can be considered dispersion magnitudes in Eqs. (3) and (4), respectively. On the other hand, the main handicaps of the 2SWEM are do not consider a non-dispersive term and to locate the bound water only at the protein surface considering that this water provokes the dispersion.

Table 3 includes the values of  $\tau_R$  obtained for our HbA and HbS samples using the LK and HK approaches as well as the 2SWEM, these values are in the same order of magnitude of those obtained using the 3SEM (Table 1). Here is remarkable the coincidence between the 3SEM and the LK method. Nevertheless, as in the case of Saturation Transfer Electronic Paramagnetic Resonance (ST-EPR)

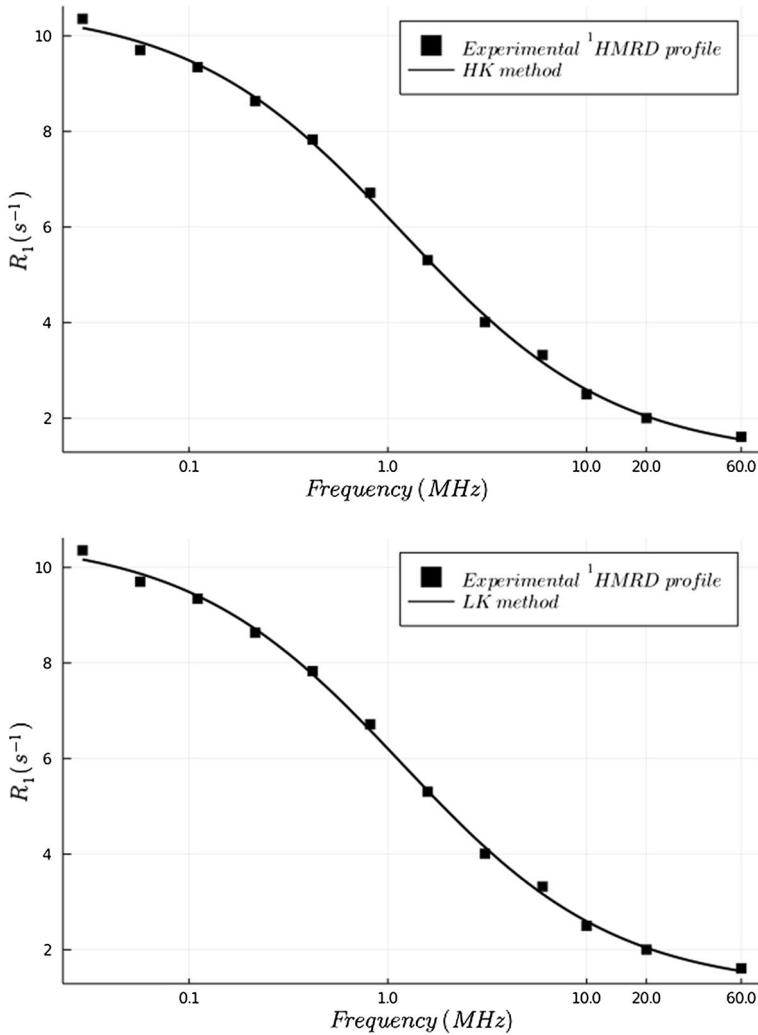


**Fig. 2** Typical  $^1\text{HMRD}$  profile of HbA and HbS intracellular solutions obtained at 310 K. The experimental results have been fitted to the LK and HK methods

measurements [18], all of these values do not match with the theoretical prediction performed by the Debye and Mooney models ( $\sim 172$  ns) for intracellular concentration and 310 K.

In spite of the increased quality of the fit achieved using the 3SEM, it is clear that it needs to be improved. For that purpose we have suggested to consider two dispersions as follow:

**Table 3** Values of  $\tau_R$  for the intracellular HbA and HbS samples used in this work (310 K) obtained using the LK and HK approaches as well as the 2SWEM

Samples	$\tau_R$ (ns.)		
	2SWEM	LK	HK
HbA-1	32.5 ± 3.0	72.7 ± 3.2	60.1 ± 0.5
HbA-2	17.5 ± 3.0	54.6 ± 4.5	41.0 ± 0.3
HbA-3	11.0 ± 0.3	81.9 ± 1.6	67.3 ± 4.6
HbA-4	14.3 ± 1.6	63.2 ± 2.0	43.4 ± 8.4
HbA-5	12.9 ± 0.5	69.8 ± 2.9	41.0 ± 2.6
HbA-6	11.1 ± 0.1	70.9 ± 3.5	41.1 ± 5.1
HbA-7	14.7 ± 0.4	89.1 ± 6.2	63.7 ± 3.4
HbS-1	26.0 ± 4.2	64.4 ± 3.5	35.7 ± 1.0
HbS-2	32.5 ± 3.0	57.3 ± 6.3	38.4 ± 7.6

$$R_1(\omega_0) = R_{1w}^{bulk} + \alpha + \beta_1 \tau_{c1} \left[ \frac{0.2}{1 + (\omega_0 \tau_{c1})^2} + \frac{0.8}{1 + 4(\omega_0 \tau_{c1})^2} \right] + \beta_2 \tau_{c2} \left[ \frac{0.2}{1 + (\omega_0 \tau_{c2})^2} + \frac{0.8}{1 + 4(\omega_0 \tau_{c2})^2} \right] \tag{5}$$

Here the subscripts 1 and 2 refer to each dispersion and  $\tau_C$  is the effective correlation time of the proton population provoking the dispersion of magnitude  $\beta$ . Figure 3 shows the fits of the typical <sup>1</sup>HMRD experimental profile, obtained in intracellular Hb solutions (310 K), to the 3SEM with one dispersion (Eq. (2)) and two

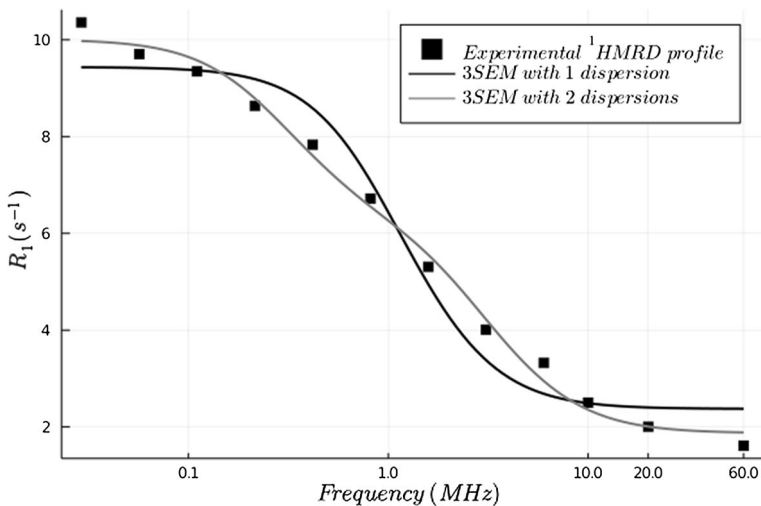


**Fig. 3** Typical <sup>1</sup>HMRD profile in intracellular Hb solutions at 310 K. The profile has been fitted using the 3SEM with 1 and 2 dispersions

dispersions (Eq. (5)), the parameters resulting of the fit to the Eq. (5) appear summarized in Table 4.

Clearly the 3SEM with two dispersions fitted the experimental  $^1\text{HMRD}$  profiles more proper than the 3SEM with only one dispersion. Two dispersions were found: one of them in the interval of frequencies from 0.3 MHz to 0.6 MHz and with correlation times in the range between 141.2 ns and 321.0 ns; and another dispersion in the interval of frequencies from 4.6 MHz to 8.4 MHz and with correlation times in the range between 11.0 ns and 20.3 ns. The correlation times associated to the first dispersion really match with the theoretical prediction for  $\tau_R$  according to the Mooney and Debye models ( $\sim 172$  ns), nevertheless, the origin of the second dispersion is unclear. In the  $^1\text{HMRD}$  profiles obtained in concentrated protein solutions, two dispersions are usually associated to the protein–protein interactions [13], nonetheless, these interactions should give place to one increased correlation time and not to one minor value as is the case in the second dispersion. Dissolved oxygen also could give place to one additional dispersion in  $^1\text{HMRD}$  [13], but this dispersion usually appear around 20 MHz and require an improved sensitivity to be observed. We suggest the second dispersion could be related to internal water molecules with  $\tau_{res}^{in} < \tau_R$ , where  $\tau_{res}^{in}$  dominates the effective correlation time ( $\frac{1}{\tau_c^{in}} = \frac{1}{\tau_{res}^{in}} + \frac{1}{\tau_R}$ ) of the dispersion. Something similar could occur with a small population of hydrated water molecules at the protein surface: more extensively hydrogen bonded than the majority of the hydrated water molecules [16], with effective correlation times higher than 1 ns and dispersing (when these molecules are present) in our frequency range of study. In any case, more deep experimental and theoretical analysis are required to define the origin of this second dispersion and this must be the subject of future works.

The Eq. (2), including or not the modification suggested in Eq. (5), is more adequate to analyze  $^1\text{H}$  magnetic relaxation during HbS polymerization than the Eq. (1) used in previous works [1, 2, 11, 12]. This physical approach describe more properly the Hb + water solution and the  $^1\text{H}$  magnetic relaxation inside it, particularly the 3SEM with two dispersions allows the proper evaluation of  $\tau_R$ . On the other hand, the  $\alpha$  and  $\beta$  values could be useful to estimate  $P_b$  behavior.

**Table 4** Parameters obtained starting from the fit of the experimental  $^1\text{HMRD}$  profiles (310 K), obtained in intracellular samples of HbA and HbS, to the 3SEM with 2 dispersions

Sample	$\alpha$ ( $\text{s}^{-1}$ )	$\beta_1$ ( $10^8 \text{ s}^{-2}$ )	$\tau_{c1}$ (ns.)	$\beta_2$ ( $10^8 \text{ s}^{-2}$ )	$\tau_{c2}$ (ns.)	Adjusted $r$ square
HbA-1	$1.32 \pm 0.02$	$0.32 \pm 0.03$	$156.3 \pm 9.3$	$2.38 \pm 0.14$	$13.5 \pm 0.9$	$0.99 \pm 0.001$
HbA-2	$1.89 \pm 0.07$	$0.24 \pm 0.04$	$141.2 \pm 28.5$	$2.17 \pm 0.39$	$14.6 \pm 3.3$	$0.99 \pm 0.002$
HbA-3	$4.24 \pm 0.04$	$0.33 \pm 0.02$	$171.5 \pm 9.0$	$3.75 \pm 0.15$	$12.3 \pm 0.5$	$0.98 \pm 0.004$
HbA-4	$2.85 \pm 0.03$	$0.28 \pm 0.04$	$167.1 \pm 15.0$	$2.96 \pm 0.43$	$12.2 \pm 1.2$	$0.98 \pm 0.006$
HbA-5	$3.40 \pm 0.03$	$0.30 \pm 0.03$	$193.0 \pm 14.0$	$4.18 \pm 0.35$	$11.0 \pm 0.8$	$0.98 \pm 0.004$
HbA-6	$3.90 \pm 0.07$	$0.22 \pm 0.03$	$230.0 \pm 33.1$	$3.03 \pm 0.17$	$14.1 \pm 1.0$	$0.98 \pm 0.004$
HbA-7	$4.44 \pm 0.07$	$0.4 \pm 0.04$	$180.5 \pm 10.1$	$3.39 \pm 0.36$	$13.6 \pm 2.0$	$0.98 \pm 0.002$
HbS-1	$1.17 \pm 0.05$	$0.15 \pm 0.02$	$202.1 \pm 21.1$	$1.82 \pm 0.20$	$16.2 \pm 1.4$	$0.98 \pm 0.003$
HbS-2	$1.70 \pm 0.04$	$0.08 \pm 0.01$	$321.0 \pm 31.0$	$1.74 \pm 0.26$	$20.3 \pm 2.7$	$0.98 \pm 0.003$



## 4 Conclusions

The three Sites Exchange Model, including the contribution of labile protons from the structure of the protein, showed to be more adequate than the two Sites Water Exchange Model to describe the  $^1\text{HMRD}$  profiles in intracellular hemoglobin solutions; the cross-relaxation contribution to the dispersion magnitude was, at least, one order of magnitude lower than the total dispersion magnitude. Two dispersions were found: one of them properly describing the hemoglobin rotational correlation time and another one probably related to internal and/or hydrated water molecules with effective correlation times higher than 1 ns and main residence times less than the protein rotational correlation time. The use of the three Sites Exchange Model creates the conditions to properly explain proton magnetic relaxation during HbS polymerization.

## Appendix 1

The two sites water exchange model (2SWEM) for  $^1\text{H}$  magnetic relaxation in protein solutions.

This approach [11–15] considers a fast exchange of water molecules between the solvent and the  $n_{ws}$  reduced amount of sites at the protein surface available for water binding. The water is considered irrotationally bound to these sites and the  $^1\text{H}$ - $^1\text{H}$  intramolecular dipolar interaction is defined as the main contribution to  $^1\text{H}$  water relaxation. Moreover, a mono-exponential autocorrelation function is used to describe the dipolar couplings and the interacting spins are considered as included in one spherical molecule rotating isotropically in a continuous media. Thus, the  $^1\text{H}$  water magnetic relaxation can be described as:

$$\begin{aligned}
 R_1(\omega_0) &= R_{1w}^{bulk} + \delta_1 \tau_C \left[ \frac{0.2}{1 + \omega_0^2 \tau_C^2} + \frac{0.8}{1 + 4\omega_0^2 \tau_C^2} \right] \\
 \delta_1 &= P_b \frac{3}{2} \left( \frac{\mu_0}{4\pi} \right)^2 \frac{\gamma^4 \hbar^2}{r^6} \\
 R_2(\omega_0) &= R_{2w}^{bulk} + \delta_2 \tau_C \left[ \frac{3}{5} + \frac{1}{1 + \omega_0^2 \tau_C^2} + \frac{0.4}{1 + 4\omega_0^2 \tau_C^2} \right] \\
 \delta_2 &= P_b \frac{3}{4} \left( \frac{\mu_0}{4\pi} \right)^2 \frac{\gamma^4 \hbar^2}{r^6}
 \end{aligned} \tag{6}$$

In the Eq. (6),  $R_2 = 1/T_2$  and  $R_{2w}^{bulk}$  is the transverse proton magnetic relaxation rate in the solvent.  $\tau_C$  is the effective correlation time of the bound water, which includes the contributions of the bound water residence time ( $\tau_{res}$ ) and  $\tau_R$  according to [16]:

$$\frac{1}{\tau_C} = \frac{1}{\tau_{res}} + \frac{1}{\tau_R} \tag{7}$$

As the bound water has been considered irrotationally bound to the protein ( $\tau_{res} > \tau_R$ ), then  $\tau_C = \tau_R$ .  $P_b$  is a function of  $n_{ws}$ , the molar concentration of Hb ( $N_{Hb}$ ), the molarity of water ( $N_w$ ) and the volume fraction occupied by the macromolecules ( $V$ ) [11, 13, 17]:

$$P_b = \frac{n_{ws} N_{Hb}}{N_w (1 - V)} \quad (8)$$

Assuming  $n_{ws} \leq 10$ , as suggested by several authors [16],  $P_b$  is in the order of  $10^{-4}$  for intracellular Hb ( $N_{Hb} = 5 \text{ mM/l}$ ) and the fraction of free water (solvent), which appears multiplying to  $R_{1w}^{bulk}$  and  $R_{2w}^{bulk}$  in the Eq. (6), can be considered equal to one.

## Appendix 2

The three sites exchange model (3SEM) for  $^1\text{H}$  magnetic relaxation in protein solutions.

The longitudinal magnetic relaxation of the  $^1\text{H}$  in aqueous solutions of proteins is dominated by the  $R_l$  of the water protons ( $R_{lw}$ ) and the labile protons at the protein structure ( $R_{lp}$ ) [1, 11, 13, 15, 16, 22]. In aqueous solutions of proteins there are three types of water: internal (in), hydrated (hy) and free (bulk) water [16, 22]. The internal water is extensively bounded to the protein, through hydrogen bonds, in small cavities and deep crevices localized at the macromolecular structure [23, 24], having main residence times ( $\tau_{res}^{in}$ ) from  $10^{-10}$  s to  $10^{-3}$  s [22–25], and rotational correlation times ( $\tau_c^{in}$ ) greater than  $10^{-9}$  s [26]. The hydrated water is bounded to the external protein surface through hydrogen bonds, having main residence times ( $\tau_{res}^{hy}$ ) and rotational correlation times ( $\tau_c^{hy}$ ) in the range from  $10^{-11}$  s to  $10^{-10}$  s [23, 25]. The free water is characterized by rotational correlation times ( $\tau_c^{bulk}$ ) in the order of  $10^{-12}$  s [16]. The labile protons are short lived protons (low values of residence times:  $\tau_{res}^p$ ) located in specific residues at the protein structure. The internal and hydrated water, as well as the labile protons, exchange fast with the solvent ( $\tau_{res}^{in}, \tau_{res}^{hy}, \tau_{res}^p \ll R_1^{-1}$ ). The  $^1\text{HMRD}$  profiles in aqueous solutions of proteins can be described using the following equation system [22]:

$$\begin{aligned}
R_1(\omega_0) &= R_{1w}^{bulk} + \alpha + \beta\tau_C \left[ \frac{0.2}{1 + (\omega_0\tau_C)^2} + \frac{0.8}{1 + 4(\omega_0\tau_C)^2} \right] \\
\alpha &= \left( \frac{N_{hy}}{N_T} \right) \left( \langle R_{1w}^{hy} \rangle_{AV} - R_{1w}^{bulk} \right) + 0.1\beta_{inter}\tau_C \\
\beta &= \beta_{intra} + 0.9\beta_{inter} + \beta_p \\
\beta_{intra} &= \frac{1}{N_T} \frac{3}{2} \sum_{\mu} \left( D_{\mu}^{intra} A_{\mu}^{intra} \right)^2 \\
\beta_{inter} &= \frac{1}{N_T} \sum_{\mu} \sum_i k_i \frac{1}{2} \left[ \left( D_{\mu 1i}^{inter} A_{\mu 1i}^{inter} \right)^2 + \left( D_{\mu 2i}^{inter} A_{\mu 2i}^{inter} \right)^2 \right] \\
D &= \left( \frac{\mu_0}{4\pi} \right) \frac{\gamma^2 \hbar}{(r_{H-H})^3} \\
\beta_p &= \frac{[R_{1p}(0) - R_{1p}(\omega_{\alpha})]}{\tau_C} \\
R_{1p}(\omega) &= \frac{1}{2(N_T + N_p)} \sum_k \frac{N_{pk}}{T_{1pk}(\omega) + (\tau_{res}^p)_k}
\end{aligned} \tag{9}$$

where  $R_{1w}^{hy}$  is the longitudinal magnetic relaxation rate of the  $^1\text{H}$  at the hydrated water molecules and the symbol  $\langle \rangle_{AV}$  is used to indicate average value.  $N_{hy}$  and  $N_{in}$  are the numbers of hydrated and internal water molecules per protein molecule.  $A$  is a generalized orientational order parameter and  $D$  is the dipole coupling constant [22].  $A_{\mu}^{intra}$  and  $D_{\mu}^{intra}$  correspond to the intramolecular dipolar interaction between the protons belonging to the internal water molecules.  $A_{\mu 1i}^{inter}$ ,  $A_{\mu 2i}^{inter}$ ,  $D_{\mu 1i}^{inter}$  and  $D_{\mu 2i}^{inter}$  correspond to the intermolecular dipolar interactions between the protons belonging to the internal water molecules and the  $i$ th proton at the macromolecular structure. Here has been considered that the  $R_1$  of the protons at the internal water molecules and the  $R_1$  of the labile protons disperse with the same effective correlation time:  $\tau_C$ .

In the Eq. (9), the  $\mu$  sum is over the  $N_{in}$  internal water molecules, the  $i$  sum is over all protons partners in long-lived intermolecular dipole couplings, the  $k$  sum is over all labile protons groups and subscripts 1 and 2 refer to the two protons at the internal water molecule [22].  $N_T$  is the total number of bound water molecules per protein molecule ( $N_T = N_{in} + N_{hy}$ ),  $N_p$  is the total number of labile protons per protein molecule and  $N_{pk}$  is the number of labile protons in each group. For intermolecular dipole couplings within the cluster of the internal water molecules  $k_i$  is a function of  $\omega_0$  and  $\tau_R$ , and for intermolecular dipole couplings with protein protons  $k_i = 1$  [22].  $\omega_{\alpha}$  is a resonance frequency at the high-frequency relaxation rate plateau. The Eq. (9) is strictly valid for an isolated pair of dipole-coupled equivalent  $I = 1/2$  nuclei.

To take into account the contribution from cross-relaxation, a negative term is added to the first equation of the Eq. (9) to obtain:

$$R_1(\omega_0) = R_{1w}^{bulk} + \alpha + \beta\tau_C \left[ \frac{0.2}{1 + (\omega_0\tau_C)^2} + \frac{0.8}{1 + 4(\omega_0\tau_C)^2} \right] - \beta_{cross}\tau_C F_{cross}(\omega_0\tau_C)$$

$$F_{cross}(\omega_0\tau_C) = \frac{\left[ \frac{1.2}{1+4(\omega_0\tau_C)^2} - 0.2 \right]^2}{\left[ 0.1 + \frac{0.3}{1+(\omega_0\tau_C)^2} + \frac{0.6}{1+4(\omega_0\tau_C)^2} \right]}$$
(10)

Here  $F_{cross}(\omega_0\tau_C)$  is obtained for the particular case in which the protons of the bound water interact with only one proton belonging to the protein structure [22]. More general and inclusive cases give place to much more complex terms describing cross-relaxation contribution with non-analytical solutions [22].

If  $\tau_{res}^{in}, \tau_{res}^p > \tau_R$ , then  $\tau_C = \tau_R$  in the equations for  $R_1, \beta_p$  and  $F_{cross}$  at the Eqs. (9) and (10) considering that:

$$\frac{1}{\tau_c^i} = \frac{1}{\tau_{res}^i} + \frac{1}{\tau_R}$$
(11)

where the superscript *i* can be referred to the internal water molecules, or to labile protons at the protein structure. In the specific case of  $\alpha$  (Eq. (9)), the second term corresponds to intermolecular dipole couplings of the internal water molecules, in which  $\tau_C = \tau_c^{in}$  is lower than 1 ns, thus contributing to the non-dispersive relaxation.

**Acknowledgements** This work was supported by the FNRS (FONDS NATIONAL DE LA RECHERCHE SCIENTIFIQUE) from Belgium, and the researchers of the NMR LABORATORY OF THE UNIVERSITY OF MONS. The authors also want to thanks to the ULB BRUSSELS UNIVERSITY HOSPITAL for its support. At the same time we want to recognize the contribution of Lissett Lores Meléndez, Cuban Student of Medicine at the INSTITUTO SUPERIOR DE CIENCIAS MÉDICAS DE SANTIAGO DE CUBA, during data processing and the writing of the manuscript. On the other hand, we really appreciate the opinions and suggestions of Professor Pascal H. Fries during manuscript revision.

**Data availability** The datasets generated during and/or analyzed during the current study are available from the corresponding author on reasonable request.

## References

1. M.A. Lores-Guevara, J.C. García-Naranjo, C.A. Cabal-Mirabal, Appl. Magn. Reson. **50**, 541 (2019). <https://doi.org/10.1007/s00723-018-1104-0>
2. C.A. Cabal-Mirabal, A. Fernández-García, M.A. Lores-Guevara, E. González-Dalmau, L. Oramas-Díaz, Appl. Magn. Reson. **49**, 589 (2018). <https://doi.org/10.1007/s00723-018-0985-2>
3. C.A. Cabal-Mirabal, M.A. Lores-Guevara, V.I. Chizhik, S.O. Rabdano, J.C. García-Naranjo, Appl Magn Reson. (2020). <https://doi.org/10.1007/s00723-020-01241-x>
4. N. Archer, F. Galacteros, C. Brugnara, Am. J. Hematol. **90**, 934 (2015). <https://doi.org/10.1002/ajh.24116>
5. L. Gravit, S. Pincock, Nature (2014). <https://doi.org/10.1038/515S1a>
6. F.B. Piel, M.H. Steinberg, D.C. Rees, N. Engl. J. Med. **376**, 1561 (2017). <https://doi.org/10.1056/NEJMra1510865>
7. E.A. Ajjack, H.A. Awooda, S.E. Adalla, Int. J. Hematol. Disord. **1**, 8 (2014). <https://doi.org/10.12691/ijhd-1-1-2>

8. L.V. Parise, N. Berliner, *Blood* **127**, 789 (2016). <https://doi.org/10.1182/blood-2015-12-674606>
9. E.I. Obeagu, K.C. Ochei, B.N. Nwachukwu, B.O. Nchuma, *Sch. J. App. Med. Sci.* **A3**, 2244 (2015)
10. A. Nowogrodzki, *Nature* **596**, S13 (2021). <https://doi.org/10.1038/d41586-021-02143-z>
11. M.A. Lores-Guevara, C.A. Cabal-Mirabal, *Appl. Magn. Reson.* **28**, 79 (2005). <https://doi.org/10.1007/BF03166995>
12. Y. Cabrales, M.A. Lores-Guevara, Y. Machado, *Appl. Magn. Reson.* **33**, 207 (2008). <https://doi.org/10.1007/s00723-008-0074-z>
13. S. Kiihne, R.G. Bryant, *Biophys. J.* **78**, 2163 (2000). [https://doi.org/10.1016/S0006-3495\(00\)76763-4](https://doi.org/10.1016/S0006-3495(00)76763-4)
14. I.R. Kleckner, M.P. Foster, *Biochim. Biophys. Acta* **1814**, 942 (2011). <https://doi.org/10.1016/j.bbapap.2010.10.012>
15. T.R. Lindstrom, S.H. Koenig, *J. Magn. Reson.* **A15**, 344 (1974)
16. B. Halle, *Phil. Trans. R. Soc. Lond. B.* **359**, 1207 (2004). <https://doi.org/10.1098/rstb.2004.1499>
17. M.A. Lores-Guevara, Y. Mengana-Torres, J.C. García-Naranjo, N. Rodríguez-Suárez, L.C. Suárez-Beyries, M.A. Marichal-Feliu, T. Simón-Boada, I.C. Rodríguez-Reyes, J. Phillipé, *Appl. Magn. Reson.* **49**, 1075 (2018). <https://doi.org/10.1007/s00723-018-1026-x>
18. M.A. Lores-Guevara, C.A. Cabal-Mirabal, O. Nascimento, A.M. Gennaro, *Appl. Magn. Reson.* **30**, 121 (2006). <https://doi.org/10.1007/BF03166986>
19. K. Hallenga, S.H. Koenig, *Biochemistry* **A15**, 4255 (1976)
20. M.A. Lores-Guevara, Y.M. Mengana-Torres, J.C. García-Naranjo, A. Ramírez-Aguilera, L.C. Suárez-Beyries, M.A. Marichal-Feliu, T. Simón-Boada, J. Phillipé, *J. Biosci. Med.* **4**, 152 (2016). <https://doi.org/10.4236/jbm.2016.412019>
21. M.A. Lores-Guevara, J.C. García-Naranjo, Y.M. Mengana-Torres, J. Pereira, *Adv. Biol. Chem.* **4**, 388 (2014). <https://doi.org/10.4236/abc.2014.46044>
22. K. Venu, V.P. Denisov, B. Halle, *J. Am. Chem. Soc.* **119**, 3122 (1997). <https://doi.org/10.1021/ja963611t>
23. V.P. Denisov, B. Halle, *Faraday Discuss.* **103**, 227 (1996). <https://doi.org/10.1039/FD9960300227>
24. V.P. Denisov, J. Peters, H.D. Hörlein, B. Halle, *Nature Struct. Biol.* **3**, 505 (1996). <https://doi.org/10.1038/nsb0696-505>
25. K. Modig, E. Liepinsh, G. Otting, B. Halle, *J. Am. Chem. Soc.* **126**, 102 (2004). <https://doi.org/10.1021/ja038325d>
26. B. Halle, V.P. Denisov, *Meth. Enzymol.* **338**, 178 (2001). [https://doi.org/10.1016/s0076-6879\(02\)38220-x](https://doi.org/10.1016/s0076-6879(02)38220-x)
27. B. Halle, H. Johanneson, K. Venu, *J. Magn. Reson.* **135**, 1 (1998). <https://doi.org/10.1006/JMRE.1998.1534>

**Publisher's Note** Springer Nature remains neutral with regard to jurisdictional claims in published maps and institutional affiliations.